Inelastic Neutron Scattering Study of Confined Surface Water on Rutile Nanoparticles

Elinor C. Spencer,[†] Andrey A. Levchenko,[‡] Nancy L. Ross,*[,†] Alexander I. Kolesnikov,[§] Juliana Boerio-Goates,[||] Brian F. Woodfield,[||] Alexandra Navrotsky,[‡] and Guangshe Li[⊥]

Department of Geosciences, Virginia Polytechnic Institute and State University, Blacksburg, Virginia 24061, Peter A. Rock Thermochemistry Laboratory and NEAT ORU, University of California at Davis, Davis, California 95616, Oak Ridge National Laboratory, P.O. BOX 2008, Oak Ridge, Tennessee 37831-6473, Department of Chemistry and Biochemistry, Brigham Young University, Provo, Utah 84602, and State Key Laboratory of Structural Chemistry, Fujian Institute of Research on the Structure of Matter, Chinese Academy of Science, Fuzhou 350002, People's Republic of China

Received: December 12, 2008; Revised Manuscript Received: January 23, 2009

The vibrational density of states (VDOS) for water confined on the surface of rutile-TiO_2 nanoparticles has been extracted from low temperature inelastic neutron scattering spectra. Two rutile-TiO_2 nanoparticle samples that differ in their respective levels of hydration, namely $TiO_2 \cdot 0.37H_2O$ (**1**) and $TiO_2 \cdot 0.22H_2O$ (**2**) have been studied. The temperature dependency of the heat capacities for the two samples has been quantified from the VDOS. The results from this study are compared with previously reported data for water confined on anatase-TiO_2 nanoparticles.

Introduction

The unique properties of metal-oxide nanoparticles has led to their proposed use in a number of commercially significant applications such as solid-state solar cells, chemical sensors, bactericidal agents, and environmental remediation.[1−7] Additionally, nanoparticles are of significance in biomineralization processes and in geological phenomena.[8,9] Fundamental to the physics of nanoparticles is the presence of surface water. This surface water in both dissociated and molecular forms plays a key role in stabilizing the nanoparticle and should be considered as an integral aspect of the particle itself.[10,11] Consequently, if a full appreciation of nanoparticle physics is to be achieved, then understanding the behavior of the confined surface water is of paramount importance.

The confinement effect is known to strongly influence both the chemistry and dynamics of water constrained within nanophase systems. By constraining water to nanoscale regions, the intricate hydrogen bond network that exists within bulk liquid water is considerably disrupted. As this network of secondary interactions is significant in that it determines the physical and chemical properties of liquid water, the perturbations caused by restricting the geometry of the aqueous environment can be extensive, and may include changes in the hydrodynamics, an alteration in the temperature dependence and structural nature of the liquid−solid phase transition, and a marked reduction in the saturation limit for common salts.[12−22]

Due to the large incoherent scattering cross-section of hydrogen and the absence of selection rules, inelastic neutron scattering (INS) techniques are invaluable for evaluating the vibrational density of states (VDOS) of water confined on the surface of metal-oxide nanoparticles.[23−25] By the judicious use of appropriate thermodynamic models, the heat capacity for the surface water can be extracted from the VDOS.[26] Recently, we reported a combined INS and adiabatic calorimetry study of water confined on the surface of anatase-TiO_2 nanoparticles.[27] Herein we report a complimentary investigation of hydrated rutile-TiO_2 nanoparticles that allows us to compare and contrast the dynamics of surface water on nanoparticles of two different TiO_2 polymorphs.

Experimental Section

Sample Preparation and Characterization. Rutile-TiO_2 nanoparticle sample **1** was prepared under hydrothermal conditions using $TiCl_4$ as the starting material. $TiCl_4$ was added to a sufficient quantity of water at 273 K with stirring to permit the hydrolysis reaction of $TiCl_4$ to $TiOCl_2$. After stirring for 2 h, a transparent solution of 2.0 M $TiOCl_2$ was formed. This solution was further diluted to 0.62 M, and 30 mL aliquots of 0.62 M $TiOCl_2$ were transferred to several Teflon-lined stainless steel autoclaves that were then put into an oven at 413 K for 2 h. When the reactions were complete, the autoclaves were allowed to cool naturally to room temperature. The final product was washed until no chloride species were detectable and then dried at 323 K in air. The phase purity of the sample was confirmed by powder X-ray diffraction (XRD) analysis. Powder XRD and magnetic data, thermogravimetric analysis (TGA), IR, UV−vis, and electron paramagnetic resonance (EPR) spectra for this sample are provided in the Supporting Information.

To prepare sample **2**, a sample of **1** was tightly wrapped in aluminum foil and placed within a heavy-walled glass evacuation tube attached to a vacuum line. The dehydration procedure was conducted in two stages. Initially the sample was placed under gentle vacuum. Once the vacuum level reached ∼100 mTorr, the level was increased by use of a Turbo-pump. At this time, the sample temperature was gradually raised to ∼373 K. Care was taken not to overheat the sample as this can cause grain coarsening. The sample was then left to dehydrate overnight under vacuum.

The rutile nanoparticles employed in this experiment are known to have a rodlike morphology.[28] The dimensions of these

* To whom correspondence should be addressed.
[†] Virginia Polytechnic Institute and State University.
[‡] University of California at Davis.
[§] Oak Ridge National Laboratory.
[||] Brigham Young University.
[⊥] Chinese Academy of Science.

10.1021/jp8109918 CCC: $40.75
Published on Web 02/25/2009

rods have been quantified by transmission electron microscopy (TEM) and are 7 nm in diameter and 35 nm in length. The particle size distribution is known to be highly uniform. The water coverage for sample **1** was determined by thermogravimetric analysis (TGA) to be 7.6 wt %. The surface area of the rutile nanoparticles, as measured by Branauer-Emmet-Teller (BET) analysis, is 96 m^2g^{-1}. Therefore, the water coverage for **1** is 4.760×10^{-5} moles of water per m^2 of rutile surface (29 molecules of water per nm^2). Consequently the chemical formula for **1** is $TiO_2 \cdot 0.37H_2O$. By measurement of the weight loss during the dehydration procedure, the water coverage for **2** was determined to be 2.817×10^{-5} moles of water per m^2 of rutile surface (17 molecules of water per nm^2). The chemical formula for **2** is therefore $TiO_2 \cdot 0.22H_2O$.

Inelastic Neutron Scattering Measurements. INS data were collected on the High Resolution Medium Energy Chopper Spectrometer (HRMECS) at the intense pulsed neutron source (Argonne National Laboratory, Argonne, Illinois).[29,30] HRMECS is a direct geometry time-of-flight instrument for which the energy of the incident neutrons (E_i) can be selected by a rotating chopper. INS spectra were collected for rutile-TiO_2 samples **1** (31.20 g) and **2** (29.83 g) at 10 and 4 K, respectively, with E_i set at 50, 140, and 600 meV, corresponding to a total energy range of $0 < E < 550$ meV and resolution of 2−3% of the incident neutron energy. The momentum transfer range (Q) was 0.75−8.4 $Å^{-1}$ and is dependent on E_i, energy transfer, and the scattering angle. Background measurements were collected with an empty sample can under similar conditions to those employed for the sample data collections. These background data were subsequently subtracted from the sample data. The measured INS data were initially transformed into dynamical structure factors, $S(Q,E)$, and then converted to the generalized vibrational density of states, $g(E)$, according to the standard expression

$$g(E) = \frac{S(Q,E)E}{Q^2[n(E,T) + 1]} \quad (1)$$

where $n(E,T)$ is the population Bose factor. The multiphonon scattering contributions were calculated with an isotropic harmonic approximation by an iterative technique with multiconvolution of the experimental spectra.[31] The resultant "single-phonon" spectra were corrected for the Debye−Waller factor.

Results and Discussion

Figure 1 shows the INS spectra for ice-Ih and for water confined on the surface of rutile nanoparticles. Due to the larger neutron scattering cross-section of hydrogen with respect to titanium and oxygen, the sample INS spectra are dominated by scattering from the hydrogen atoms associated with the water located on the surface of the rutile nanoparticles. Furthermore, in the case of optical vibrations the scattering intensity is inversely proportional to the mass of the vibrating atom.[32]

The low energy translational band of ice-Ih is located in the 0−40 meV range (Figure 1A), whereas the band in the 50−120 meV region corresponds to the librational motions of the water molecules (Figure 1B).[33] The first acoustic peak observed at 7 meV in the ice-Ih spectrum is absent in both hydrated rutile spectra. In addition, the other translational peaks within the rutile spectra are broadly distributed at higher energies with respect to ice-Ih. This energy redistribution is indicative of suppression of the low energy translational motion of the confined water molecules due to strong hydrogen bond interactions between the water and the surface of the TiO_2 nanoparticles; similar

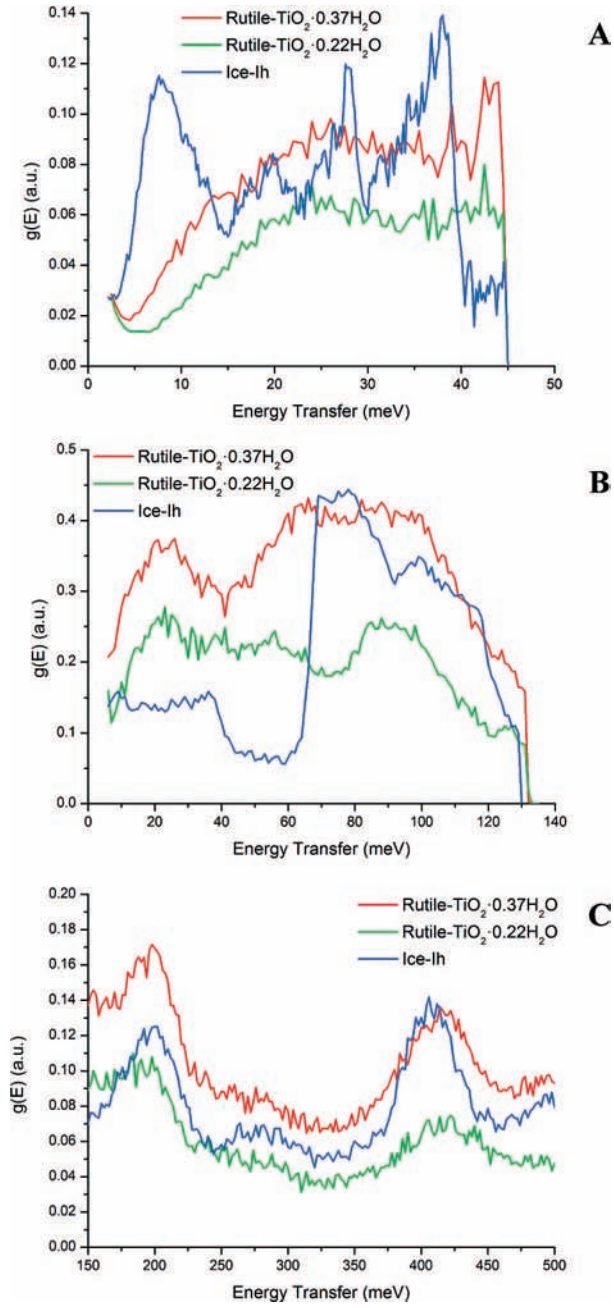

Figure 1. INS spectra of ice-Ih and water on rutile nanoparticles. (A) $E_i = 50$ meV; (B) $E_i = 140$ meV; (C) $E_i = 600$ meV.

behavior has been reported for water confined on anatase-TiO_2 nanoparticles.[27]

If the INS spectra in the 0−45 meV range (Figure 1A) for **1** and **2** are scaled such that their total integrated areas are equal, then **1** has a greater intensity in the 6−16 meV energy range with respect to **2**. This indicates an overall softening of the acoustic vibrations of the water molecules with increasing hydration level. The translational bands in the INS spectra for **1** and **2** have a similar structure above 16 meV.

As noted above, the bands in the 50−120 meV region of the spectra represent the librational motions of the water molecules (Figure 1B). There are no vibrational modes observed in the ice-Ih spectrum within the energy range of 40−65 meV, and the librational band for ice-Ih is restricted to the 65−120 meV range with broad peaks appearing at approximately 75 and 105 meV. Conversely, within the hydrated rutile spectra the librational bands are broadly distributed over the 40−120 meV

energy range. The librational motion (restricted rotational movement) of the water molecules is strongly influenced by the arrangement and extent of the intermolecular interactions in which they participate. The nonexistence of distinct peaks within the librational region of hydrated rutile spectra and the presence of librational bands in the 40−65 meV region that are absent in the ice-Ih spectrum are suggestive of redistribution of the librational energy of the water molecules confined on the surface of the rutile nanoparticles and possible disorder and weakening of the hydrogen bonds between the water molecules. It is possible the vibrations of the hydrogen atoms associated with the physisorbed water molecules and surface-bound hydroxyl groups are correlated with the intense optical modes of the TiO_2 lattice that are prevalent within the 35−65 meV energy range, and consequently there is a significant contribution of these riding modes to the INS spectrum at these energies. The broad peak at 45−65 meV in the INS spectrum for **2** that is not well developed in the spectrum for **1**, supports this hypothesis. These findings are congruent with the INS spectral results reported for hydrated anatase.

The center of gravity (CoG) for the librational regions in the ice-Ih and hydrated rutile INS spectra were calculated using the following equation:

$$\mathrm{CoG} = \frac{\int_a^b E \cdot \mathrm{g}(E)^P + \mathrm{d}E}{\int_a^b \mathrm{g}(E)^P \mathrm{d}E} \qquad (2)$$

where a = lower limit of the librational energy range, b = upper limit of the librational energy range, and P = weighting parameter. In this case, a = 50 meV and b = 120 meV; the parameter P was set such that the weighting is against the absolute spectrum (P = 1). The CoG values for the librational bands of ice-Ih and of hydrated rutile were calculated to be 88.9 and 83.4 (**1**) and 83.1 meV (**2**), respectively. The shift of the CoG to lower energy for the surface water with respect to ice-Ih [ΔE = 5.5 (**1**) and 5.8 meV (**2**)] reveals an overall softening of the intermolecular hydrogen bond environment for the confined water that may be related to a distortion of the water tetrahedra.[34−36]

The higher energy regions of the INS spectra (Figure 1C) relate to the bending and stretching modes of the molecular water and surface hydroxyl groups. The peaks at 200 and ∼410 meV that are present in both the ice-Ih and hydrated rutile spectra are assigned to the H−O−H bending and O−H stretching modes of the molecular water, respectively. The peaks at 412 and 416 meV in the spectra for **1** and **2**, respectively, are at a higher energy than the corresponding peak at 406 meV in the ice-Ih spectrum (peak positions were obtained by fitting the peaks with a Gaussian function). These energy shifts suggest hardening of the O−H stretching for the molecular water residing on the surface of the rutile nanoparticles. This would occur for water molecules possessing strong O−H covalent bonds resulting from the formation of weak hydrogen bonds, presumably with the surface-bound hydroxyl groups. Moreover, the full width at half-maximum (fwhm) values for the O−H stretching peaks are 50, 60, and 43 meV for **1**, **2**, and ice-Ih, respectively, suggesting a wider distribution of O−H covalent bond strengths for the surface confined water compared to water molecules in ice-Ih.

In contrast to the INS spectrum of hydrated anatase, no peak at ∼450 meV is observed within the hydrated rutile spectra. This peak in the anatase spectrum is superposed on the peak at

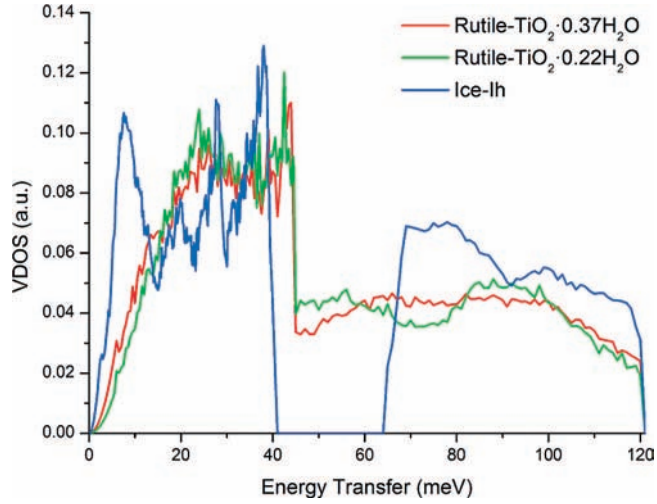

Figure 2. Vibrational density of states for hydrated rutile nanoparticles and ice-Ih. Only the VDOS in the energy ranges corresponding to the librational and translational bands are shown.

400 meV and is associated with the O−H stretching motion of the surface hydroxyl groups, or stretching of the non-hydrogen bonded molecular water. The absence of this peak in the hydrated rutile spectra would imply either a deficiency of such groups on the surface of the rutile nanoparticles with respect to anatase or, more likely, this peak may be masked in the hydrated rutile spectra by the broad peaks at 412 (**1**) and 416 meV (**2**) due to the higher levels of hydration of the rutile samples used in this INS experiment compared to the anatase INS sample (29, 17, and 9 water molecules per nm^2 of TiO_2 surface for **1**, **2** and anatase, respectively).

The VDOS for the surface water can be obtained by normalization of the generalized vibrational density of states spectra [g(E)]. The normalization procedure requires that the total areas of librational and translational bands of water both be equal to three, corresponding to the three degrees of freedom for each of the translational and librational modes of water. Additionally, the low energy region of the spectrum must be modeled by the Debye approximation, $\mathrm{g}(E) \approx AE^2$, where A is a constant that is inversely proportional to the cube of the Debye frequency.[37,38] The VDOS for **1** and **2** are shown in Figure 2, and for comparison the VDOS spectrum for ice-Ih is also shown in this figure.

The isochoric heat capacity (C_v) can be extracted from the VDOS spectrum by use of the following expression:[26]

$$C_v = \int_0^\infty \frac{\mathrm{g}(\omega)(\hbar\omega/kT)^2 \exp(\hbar\omega/kT)}{[\exp(\hbar\omega/kT) - 1]^2} \mathrm{d}\omega \qquad (3)$$

where $\hbar$ is Dirac's constant (reduced Planck's constant), ω is the phonon angular frequency, k is Boltzmann's constant, and T is the temperature.

The isochoric heat capacity is related to the isobaric heat capacity (C_p) by $C_p = TV\alpha^2/\beta + C_v$, where V is the molar volume, α is the volumetric coefficient of thermal expansion, and β is the isothermal compressibility.[39] Klug et al. calculated the first term on the right-hand side of this equation to be 0.025 J K^{-1} mol^{-1} at 100 K for ice-**I**.[26] As this value is negligible, we can assume that $C_p = C_v$.[40]

Heat capacity versus temperature curves for ice-Ih and confined water calculated from the INS VDOS spectra are shown in Figure 3. For the purpose of comparison, the C_v curve

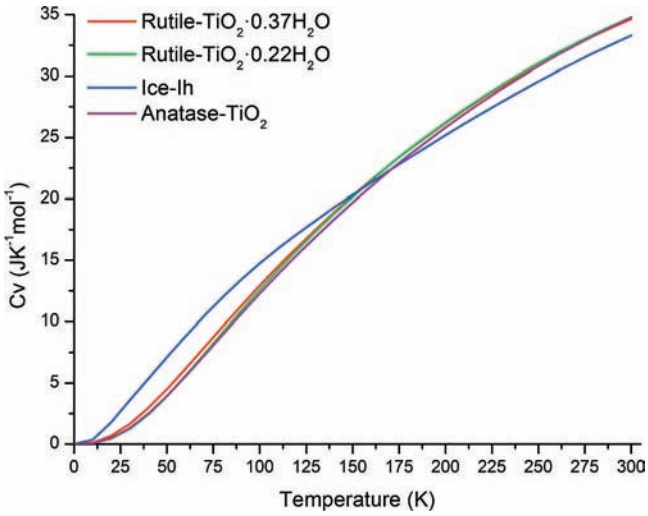

Figure 3. C_v data for ice-Ih and hydrated rutile nanoparticles as calculated from the INS VDOS data. Anatase data taken from ref 27.

for hydrated anatase nanoparticles, as calculated from INS data, is also shown in this figure.

The C_v curves for confined water obtained from the VDOS spectra are lower than that of ice-Ih at low temperatures but greater at higher temperatures with the crossover point being between 160−170 K. This crossover can be ascribed to the contribution to the heat capacity from the additional librational bands between 40−65 meV in the INS spectra for hydrated rutile that are absent in the ice-Ih spectrum. The C_v curves for hydrated rutile are almost identical to the anatase C_v curve, implying that the average heat capacity for water confined on the surface of TiO_2 nanoparticles is insensitive to the polymorphism of the underlying metal-oxide particle. The only significant difference between the C_v curves for the two polymorphs is in the crossover temperature, which is lower for water on rutile with respect to water on anatase (∼180 K). This is consistent with the results from calorimetric experiments.[28]

It should be noted that the C_v curves presented herein are calculated from INS data and represent average molar heat capacities, whereas the heat capacity curves published by Boerio-Goates et al.[28] for the various hydration layers on rutile-TiO_2 nanoparticles correspond to difference data. Consequently, the data from these two techniques cannot be compared directly.

The vibrational entropy (S) can be calculated from the heat capacity curves using the following equation:[38]

$$S = \int_0^T \frac{C_p}{T}\,dT \qquad (4)$$

In this case we are assuming $C_p = C_v$, and therefore the entropy values at 298 K based on the C_v curves derived from the INS data for ice-Ih and for water confined on the surface of rutile nanoparticles are 37.08, 32.89 (**1**), and 32.34 J K^{-1} mol^{-1} (**2**), respectively. As the lower temperature heat capacities contribute significantly to the entropy, the reduction in the entropy of the surface water with respect to ice-Ih [$\Delta S = -4.19$ (**1**) and -4.74 J K^{-1} mol^{-1} (**2**)] may be attributed to the diminished heat capacity of hydration layer at these temperatures (Figure 3). These entropy values calculated from the INS data are marginally lower than the values reported for ice-Ih and for water on anatase nanoparticles obtained from low temperature adiabatic calorimetry measurements (41.54 and 37.07 J K^{-1} mol^{-1} for ice-Ih and water confined on anatase nanoparticles, respectively).[27] However, the difference in entropy between the hydration layer on anatase and ice-Ih ($\Delta S = -4.47$ J $K^{-1}mol^{-1}$) is comparable to differences reported above for the hydrated rutile systems. The decrease in the vibrational entropy with respect to ice-Ih for water confined on both anatase and rutile nanoparticles reflects an overall restriction of the vibrational motion exhibited by the water molecules, possibly due to their interaction with the TiO_2 surface.

Conclusion

INS spectra of water confined on the surface of rutile-TiO_2 nanoparticles have been reported. Two rutile-TiO_2 nanoparticle samples with different levels of hydration were employed in this study: $TiO_2 \cdot 0.37H_2O$ (**1**) and $TiO_2 \cdot 0.22H_2O$ (**2**). This analysis allowed for an evaluation of the hydrodynamics of the confined water, which were found to be influenced strongly by the intermolecular interactions between the water and the nanoparticle surface. The VDOS were calculated from the INS spectra, and the heat capacity for the surface water layers as a function of temperature were elucidated. The vibrational entropy values for the nanoparticle hydration layers were then calculated from the heat capacity curve to be 32.89 (**1**) and 32.34 J K^{-1} mol^{-1} (**2**). Interesting, the level of hydration does not appear to have a significant influence on the thermodynamic properties of the hydrated rutile-TiO_2 nanoparticles. The results from this investigation were compared to previously reported INS data for water confined on anatase-TiO_2 nanoparticles. It is apparent that thermodynamic properties, as derived from INS data, for the hydration layers on nanoparticles of these two polymorphs show a high degree of similarity.

Acknowledgment. N.L.R., E.C.S., and A.A.L. acknowledge support from the U.S. Department of Energy, Office of Basic Energy Sciences (DOE-BES), Grant DE FG03 01ER15237. A.I.K. wishes to acknowledge ORNL/SNS that is managed by UT-Battelle, LLC, for DOE under Contract DE-AC05-00OR22725. Argonne National Laboratory is supported by DOE-BES under contract DE-AC02-06CH11357. We are thankful to L. Jirik for assistance with the INS experiments conducted at the IPNS.

Supporting Information Available: Powder XRD spectra, magnetic data, adsorption data, TGA, IR, UV−vis, and EPR spectra for sample **1**. This material is available free of charge via the Internet at http://pubs.acs.org.

References and Notes

(1) Franke, M. E.; Koplin, T. J.; Simon, U. *Small* **2006**, *2* (1), 36.
(2) Beek, W. J. E.; Wienk, M. M.; Janssen, R. A. J. *Adv. Mater.* **2004**, *16* (12), 1009.
(3) Stoimenov, P. K.; Klinger, R. L.; Marchin, G. L.; Klabunde, K. J. *Langmuir* **2002**, *18*, 6679.
(4) Oskam, G. *J. Sol-Ge. Sci. Technol.* **2006**, *37*, 161.
(5) Vayssieres, L.; Hagfeldt, A.; Lindquist, S. E. *Pure Appl. Chem.* **2000**, *72* (1), 47.
(6) Luo, X.; Morrin, A.; Killard, A. J.; Smyth, M. R. *Electroanalysis* **2006**, *18* (4), 319.
(7) Rickerby, D. G.; Morrison, M. *Sci. Technol. Adv. Mater.* **2007**, *8*, 19.
(8) Navrotsky, A. *Proc. Natl. Acad. Sci.* **2004**, *101* (33), 12096.
(9) Navrotsky, A. *Geochem. Trans.* **2003**, *4* (6), 34.
(10) Li, G.; Li, L.; Boerio-Goates, J.; Woodfield, B. F. *J. Am. Chem. Soc.* **2005**, *127*, 8659.
(11) Levchenko, A. A.; Li, G.; Boerio-Goates, J.; Woodfield, B. F.; Navrotsky, A. *Chem. Mater.* **2006**, *18*, 6324.
(12) Alcoutlabi, M.; Mckenna, G. B. *J. Phys.: Condens. Matter.* **2006**, *17*, R461.

(13) Rasaiah, J. C.; Garde, S.; Hummer, G. *Annu. Rev. Phys. Chem.* **2008**, *59*, 713.

(14) Crupi, V.; Dianoux, A. J.; Majolino, D.; Migliardo, P.; Venuti, V. *Phys. Chem. Chem. Phys.* **2002**, *4*, 2768.

(15) Malani, A.; Ayappa, K. G.; Murad, S. *Chem. Phys. Lett.* **2006**, *431*, 88.

(16) Crupi, V.; Majolino, D.; Migliardo, P.; Venuti, V. *J. Mol. Liq.* **2005**, *117*, 165.

(17) Kolesnikov, A. I.; Zanotti, J.-M.; Loong, C.-K.; Thiyagarajan, P. *Phys. Rev. Lett.* **2004**, *93* (3), 035503.

(18) Moilanen, D. E.; Levinger, N. E.; Spry, D. B.; Fayer, M. D. *J. Am. Chem. Soc.* **2007**, *129*, 14311.

(19) Crupi, V.; Longo, F.; Majolino, D.; Venuti, V. *Eur. Phys. J. Spec. Top.* **2007**, *141*, 61.

(20) Alba-Simionesco, C.; Coasne, B.; Dosseh, G.; Dudziak, G.; Gubbins, K. E.; Radhakrishnan, R.; Sliwinska-Bartkowiak, M. *J. Phys.: Condens. Matter.* **2006**, *18*, R15.

(21) Raviv, U.; Laurat, P.; Klein, J. *Nature* **2001**, *413*, 51.

(22) Mamontov, E.; Wesolowski, D. J.; Vlcek, L.; Cummings, P. T.; Rosenqvist, J.; Wang, W.; Cole, D. R. *J. Phys. Chem. C* **2008**, *112*, 12334.

(23) Loong, C.-K.; Iton, L. E.; Ozawa, M. *Phys. B* **1995**, *213*, 640.

(24) Loong, C.-K.; Richardson, J. W.; Ozawa, M. *J. Catal.* **1995**, *157*, 636.

(25) Mitchell P. C. H.; Parker, S. F.; Ramirez-Cuesta, A. J.; Tomkinson J. *Vibrational Spectroscopy with Neutrons with Applications in Chemistry, Biology, Materials Science and Catalysis*; World Scientific Publishing Co. Pte. Ltd.: River Edge, NJ, 2005.

(26) Klug, D. D.; Whalley, E.; Svensson, E. C.; Root, J. H.; Sears, V. F. *Phys. Rev. B* **1991**, *44* (2), 841.

(27) Levchenko, A. A.; Kolesnikov, A. I.; Ross, N. L.; Boerio-Goates, J.; Woodfield, B. F.; Li, G.; Navrotsky, A. *J. Phys. Chem. A* **2007**, *111*, 12584.

(28) Boerio-Goates, J.; Li, G.; Li, L.; Walker, T. F.; Parry, T.; Woodfield, B. F. *Nano Lett.* **2006**, *6* (4), 750.

(29) Loong, C.-K.; Ikeda, S.; Carpenter, J. M. *Nucl. Instrum. Methods Phys. Res.* **1987**, *A260*, 381.

(30) Kolesnikov, A. I.; Zanotti, J.-M.; Loong, C.-K. *Neutron News* **2004**, *15* (3), 19.

(31) Kolesnikov, A. I.; Natkaniec, I.; Antonov, V. E.; Belash, I. T.; Fedotov, V. K.; Krawczyk, J.; Mayer, J.; Ponyatovsky, E. G. *Phys. B* **1991**, *174*, 257.

(32) The coherent (σ_{coh}), incoherent (σ_{inc}), and total (σ_{tot}) neutron scattering cross-sections for hydrogen are 1.76, 80.26, and 82.02 barns, respectively. For titanium $\sigma_{coh} = 1.48$ barns, $\sigma_{inc} = 2.87$ barns, and $\sigma_{tot} = 4.35$ barns. For oxygen $\sigma_{coh} = 4.23$ barns, $\sigma_{inc} = 0.00$ barns, and $\sigma_{tot} = 4.23$ barns. These values are taken from Sears, V. F. *Neutron News* **1992**, *3*, 26.

(33) Li, J.; Kolesnikov, A. I. *J. Mol. Liq.* **2002**, *100*, 1.

(34) Guillot, B.; Guissani, Y. *J. Chem. Phys.* **2003**, *119* (22), 11740.

(35) Kolesnikov, A. I.; Li, J.-C.; Dong, S.; Bailey, I. F.; Eccleston, R. S.; Hahn, W.; Parker, S. F. *Phys. Rev. Lett.* **1997**, *79* (10), 1869.

(36) Klug, D. D.; Tulk, C. A.; Svensson, E. C.; Loong, C.-K. *Phys. Rev. Lett.* **1999**, *83* (13), 2584.

(37) Kieffer, S. W. *Rev. Geophys. Space Phys.* **1979**, *17* (1), 1.

(38) Richet, P. *The Physical Basis of Thermodynamics with Applications to Chemistry*; Kluwer Academic/Plenum Publishers: Norwell, MA, 2001.

(39) Tanaka, H. *J. Mol. Liq.* **2001**, *90*, 323.

(40) Johari, G. P.; Andersson, O. *Phys. Rev. B* **2006**, *73*, 094202.

JP8109918